

Synthesis and Oxidation of Iron(II) Ferrocenylacetylide Diphosphine Complexes. A Novel Type of Mixed-Valence Complex

Masaru Sato* and Yukiko Hayashi

Chemical Analysis Center, Saitama University, Urawa, Saitama 338, Japan

Shigekazu Kumakura and Natsuko Shimizu

Department of Chemistry, Faculty of Science, Saitama University, Urawa 338, Japan

Motomi Katada and Satoshi Kawata

Department of Chemistry, Faculty of Science, Tokyo Metropolitan University, Hachioji-shi, Tokyo, Japan

Received July 10, 1995[®]

Some Fe(II) ferrocenylacetylide complexes, [(Cp or Cp*)(PP)FeC≡CFC], were prepared by the photolysis of the corresponding carbonyl complexes [(Cp or Cp*)(CO)₂FeC≡CFC] in the presence of diphosphines (PP = dppe, dppm, dmpe). The cyclic voltammograms showed two quasi-reversible waves at −0.47 to −0.84 and +0.08 to +0.12 V. The one-electron-oxidized species were isolated as relatively stable solids from the reaction of the neutral Fe(II) complexes with DDQ or FcHPF₆. The oxidized complexes exhibited an intervalence transfer band at 1295–1595 nm, and the interaction parameters were calculated from the position ($\alpha^2 = (0.98–2.44) \times 10^{-2}$). This suggests that these are highly electron delocalized mixed-valence complexes. The IR spectra ($\nu_{\text{CC}} = 1956–1976 \text{ cm}^{-1}$), the ESR spectra (appearance of one broad signal), and the Mössbauer spectra ($QS = 2.00–2.26 \text{ mm s}^{-1}$) support the above suggestion. The structure of [Cp(dppe)FeC≡CFC] was determined by single-crystal X-ray diffraction.

Introduction

Mixed-valence complexes are of interest for the investigation of electron-transfer processes, for their enormous potential in the production of new materials with super- and semiconductivity, and for their relevance to biologically important systems.¹ In organometallic chemistry, since Cowan and his co-workers reported the monocation of biferrocene,² a great number of binuclear ferrocene derivatives have been prepared and the oxidized species have been investigated extensively.³ Recently, mixed-valence systems of (η -C₅R₅)L₂-Fe^{−4} and other organoiron derivatives⁵ also have been reported. However, few binuclear complexes containing two iron atoms with each in a different coordination mode have been prepared.⁶ In such complexes we can

gain more insight into the factors which affect the extent of electron delocalization in mixed-valence complexes: the mode of coordination to a metal, the kind of ligands, and so on. In our latest report, we described the synthesis and properties of some Fe(II) ferrocenylacetylide complexes and the corresponding oxidized species.⁷ In recent years, some transition-metal ferrocenylacetylide complexes also were investigated from the same⁸ or other viewpoints (e.g., nonlinear optics).^{9,10} Herein, we extend our system to include the synthesis of a complex with a phosphine ligand, [(Cp or Cp*)Fe(PP)(C≡CFC)], and their one-electron-oxidized species.

[®] Abstract published in *Advance ACS Abstracts*, December 15, 1995.

(1) (a) *Mixed-Valence Compounds*; Brown, D. B., Ed.; D. Reidel: Boston, MA, 1980. (b) Astruc, D. *Electron-Transfer and Radical Processes in Transition Metal Chemistry*; VCH: New York, 1995; Chapter 1.

(2) Cowan, D. O.; Kaufman, F. *J. Am. Chem. Soc.* **1970**, *92*, 219. Kaufman, F.; Cowan, D. O. *J. Am. Chem. Soc.* **1970**, *92*, 6198.

(3) (a) Zhang, W.; Wilson, S. R.; Hendrickson, D. N. *Inorg. Chem.* **1989**, *28*, 4160 and references therein. (b) Dong, T.-Y.; Ke, T.-J.; Peng, S.-M.; Yeh, S.-K. *Inorg. Chem.* **1989**, *28*, 2103. (c) Talham, D. R.; Cowan, D. O. *Organometallics* **1987**, *6*, 932. (d) Amer, S. I.; Sadler, G.; Henry, R. M.; Ferguson, G.; Ruhl, B. L. *Inorg. Chem.* **1985**, *24*, 1517. (e) Lee, M.-T.; Foxman, B. M.; Rosenblum, M. *Organometallics* **1985**, *4*, 539.

(4) (a) Delville, M.-H.; Lacoste, M.; Astruc, D. *J. Am. Chem. Soc.* **1992**, *114*, 8310. (b) Chukwu, R.; Hunter, A. D.; Santarsiero, B. D. *Organometallics* **1992**, *11*, 589. (c) Le Narvor, N.; Lapinte, C. *Organometallics* **1993**, *12*, 357. (d) Etzenhouser, B. A.; Cavanaugh, M. D.; Spurgeon, H. N.; Sponsler, M. B. *J. Am. Chem. Soc.* **1994**, *116*, 2221. (e) Etzenhouser, B. A.; Chen, Q.; Sponsler, M. B. *Organometallics* **1994**, *13*, 4176.

(5) (a) Delville, M.-H.; Rittinger, S.; Astruc, D. *J. Chem. Soc., Chem. Commun.* **1992**, 519. (b) Stephan, M.; Davis, J. H.; Meng, X.; Chase, K. J.; Hauss, J.; Zenneck, U.; Pritzkow, H.; Siebert, W.; Grimes, R. N. *J. Am. Chem. Soc.* **1992**, *114*, 5214.

(6) (a) Guerchais, V. *J. Chem. Soc., Chem. Commun.* **1990**, 534. (b) Liu, L.-K.; Luh, L.-S. *Organometallics* **1994**, *13*, 2816. (c) Osborne, A. G.; Whiteley, R. H. *J. Organomet. Chem.* **1979**, *181*, 425. (d) Pannell, K. H.; Cassias, J. B.; Crawford, G. M.; Flores, A. *Inorg. Chem.* **1976**, *15*, 2671.

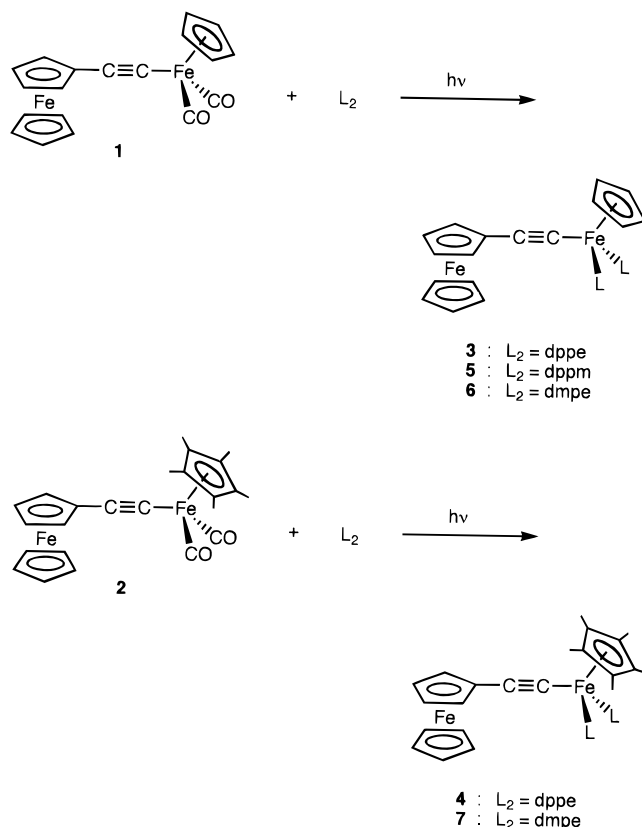
(7) Sato, M.; Hayashi, Y.; Katada, M.; Kawata, S. *J. Organomet. Chem.* **1994**, *471*, 179.

(8) (a) Sato, M.; Shintate, H.; Kawata, Y.; Sekino, M.; Katada, M.; Kawata, S. *Organometallics* **1994**, *13*, 1956. (b) Sato, M.; Mogi, E.; Kumakura, S. *Organometallics* **1995**, *14*, 3157. (c) Sato, M.; Mogi, E.; Katada, M. *Organometallics* **1995**, *14*, 4837.

(9) (a) Colbert, M. C. B.; Ingham, S. L.; Lewis, J.; Long, N. J.; Raithby, P. R. *J. Chem. Soc., Dalton Trans.* **1994**, 2215. (b) Colbert, M. C. B.; Edwards, A. J.; Lewis, J.; Long, N. J.; Page, N. A.; Parker, D. G.; Raithby, P. R. *J. Chem. Soc., Dalton Trans.* **1994**, 2589.

(10) (a) Bunz, U. H. F.; Enkelmann, V. *Organometallics* **1994**, *13*, 3823. (b) Koridze, A. A.; Yanovsky, A. I.; Struchkov, Yu. T. *J. Organomet. Chem.* **1992**, *441*, 277. (c) Russo, M. V.; Furlani, A.; Licocchia, S.; Paolesse, R.; Villa, A. C.; Guastini, C. *J. Organomet. Chem.* **1994**, *469*, 245. (d) Onitsuka, K.; Tao, X.-Q.; Sonogashira, K. *Bull. Chem. Soc. Jpn.* **1994**, *67*, 2611. (e) Weigand, W.; Robl, C. *Chem. Ber.* **1993**, *126*, 1807.

Scheme 1



Results and Discussion

Syntheses and Characterization. The key starting materials are $\text{Cp}(\text{CO})_2\text{FeC}\equiv\text{CFc}$ (**1**) and $\text{Cp}^*(\text{CO})_2\text{FeC}\equiv\text{CFc}$ (**2**) ($\text{Cp} = \eta\text{-C}_5\text{H}_5$ and $\text{Cp}^* = \eta\text{-C}_5\text{Me}_5$), which were reported in a previous paper.⁷ A yellow solution of **1** in acetonitrile was irradiated with a 100 W high-pressure Hg lamp to give the thermally stable complex $\text{Cp}(\text{dppe})\text{FeC}\equiv\text{CFc}$ (**3**), in 71% yield (dppe = bis(diphenylphosphino)ethane). $\text{Cp}(\text{dppm})\text{FeC}\equiv\text{CFc}$ (**5**) and $\text{Cp}(\text{dmpe})\text{FeC}\equiv\text{CFc}$ (**6**) were prepared similarly (dppm = bis(diphenylphosphino)methane and dmpe = bis(dimethylphosphino)ethane). $\text{Cp}^*(\text{dppe})\text{FeC}\equiv\text{CFc}$ (**4**) and $\text{Cp}^*(\text{dmpe})\text{FeC}\equiv\text{CFc}$ (**7**) were obtained in moderate yield from the photolysis of **2** with dppe and dmpe, respectively, in the same manner as for the Cp series. Generally, the photolysis of carbonyl complexes with a Cp ligand has been used extensively as an efficient method to obtain other carbonyl-free species, but there are only a few successful examples in which an Fp^* diphos compound has thus been prepared.¹¹ Accordingly, it is worth noting that complexes **3–7** are readily prepared by photoirradiation. In addition, complex **3** could be prepared by the reaction of $\text{FcC}\equiv\text{CLi}$ with $\text{Cp}(\text{dppe})\text{FeI}$ in 64% yield, but complex **4** could not be isolated in a similar reaction. The composition and structures of these complexes were determined by elemental analyses and IR and ^1H and ^{13}C NMR spectra. For example, in the IR spectrum of **7**, the $\text{C}\equiv\text{C}$ stretching vibration was observed at 2044 cm^{-1} . The ^1H NMR spectrum (C_6D_6) of **7** exhibited signals assigned to the ferrocenyl ring protons at δ 3.98 (2H), 4.29 (2H),

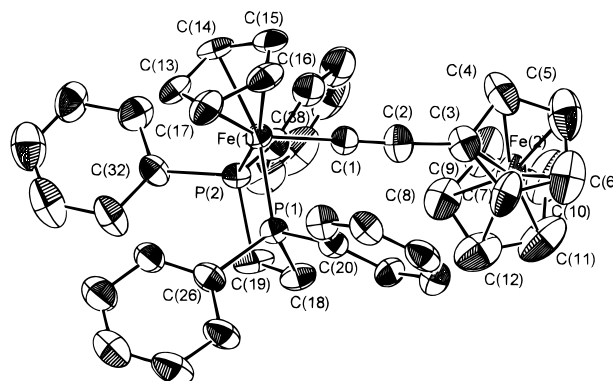


Figure 1. ORTEP view for one of the molecules of complex **3**.

Table 1. Selected Bond Distances and Bond Angles for Complex **3**

Bond Distances (Å)			
Fe(1)–P(1)	2.159(3)	Fe(1)–P(2)	2.155(3)
Fe(1)–C(1)	1.190(11)	Fe(1)–C(13)	2.094(12)
Fe(1)–C(14)	2.111(12)	Fe(1)–C(15)	2.119(10)
Fe(1)–C(16)	2.122(12)	Fe(1)–C(17)	2.110(13)
C(1)–C(2)	1.196(16)	C(2)–C(3)	1.455(17)
Bond Angles (deg)			
P(1)–Fe(1)–P(2)	86.7(2)	P(1)–Fe(1)–C(1)	89.9(4)
P(2)–Fe(1)–C(1)	83.1(4)	Fe(1)–C(1)–C(2)	177.0(9)
C(1)–C(2)–C(3)	176.4(12)	Fe(2)–C(3)–C(2)	126.2(8)

and 4.26 (5H), the methyl protons of the Cp^* ring at δ 1.75 (15H), those of dmpe at δ 0.95 (6H) and 1.49 (6H), and the methylene protons of dmpe at δ 1.03 (2H) and 1.90 (2H). In the ^{13}C NMR spectrum (C_6D_6) of **7**, signals due to the ferrocenyl ring carbons appeared at δ 66.33, 69.37, 69.91, and 70.51, the ring carbons of Cp^* at δ 86.40, the methyl carbons of Cp^* at 11.10, those of dmpe at δ 16.84 and 18.42, the methylene carbons of dmpe at δ 30.02, and the acetylene carbons at δ 77.50 and 108.10.

Structure. For complex **3**, a single-crystal X-ray diffraction study was carried out to confirm the structure. The crystal, which was obtained by recrystallization from $\text{CH}_2\text{Cl}_2/\text{hexane}$, contained two independent molecules in its unit cell. Because of the large disorder in the cyclopentadienyl rings of the ferrocene moiety in one of the molecules, the ORTEP view and the selected structural data of only one molecule are offered in Figure 1 and Table 1, respectively. Ferrocenylacetylene is bonded at the terminal carbon to the iron atom in the $\text{Cp}(\text{dppe})\text{Fe}$ part. The Fe–C(1) distance is 1.910 Å, which is similar to that in other Fe acetylides (e.g. 1.900(7) Å in $\text{Cp}(\text{dppm})\text{FeC}\equiv\text{CPh}$,¹² 1.920(6) Å in $\text{Cp}(\text{CO})_2\text{FeC}\equiv\text{CPh}$ ¹³). The ferrocenylacetylide ligand is bonded almost linearly to the metal (Fe–C(1)–C(2), $177.0(9)^\circ$; C(1)–C(2)–C(3), $176.4(12)^\circ$). The C(1)–C(2) distance (1.196(16) Å) remains in the range for $\text{C}\equiv\text{C}$ bond lengths in metal acetylide complexes (1.18–1.24 Å).¹⁴ The coordination around the Fe atom of the Cp ligand, the two P atoms of the chelating dppe molecule, and the terminal carbon C(1) of the ferrocenylacetylide ligand can be described as a three-legged piano stool. The angle involving the two phosphine-containing legs, P(1)–Fe(1)–P(2) ($86.7(2)^\circ$), is significantly larger than

(11) (a) Ruiz, J.; Román, E.; Astruc, D. *J. Organomet. Chem.* **1987**, 322, C13. (b) Roger, C.; Hamon, P.; Toupet, L.; Rabaa, H.; Saillard, J.-Y.; Hamon, J.-R.; Lapinte, C. *Organometallics* **1991**, 10, 1045.

(12) Camesa, M. P.; Gimeno, J.; Lastra, E.; Lanfranchi, M.; Tiripicchio, A. *J. Organomet. Chem.* **1991**, 405, 333.

(13) Goddard, R.; Howard, J.; Woodward, P. J. *J. Chem. Soc., Dalton Trans.* **1974**, 2025.

(14) Nast, R. *Coord. Chem. Rev.* **1982**, 47, 89.

Table 2. Redox Potentials (V) of Complexes 3–7 in 0.1 M (*n*-Bu)₄NClO₄/CH₂Cl₂ at 0.1 V s⁻¹ (vs FcH/FcH⁺)^a

compd	<i>E</i> _{1/2} (1)	<i>E</i> _{1/2} (2)
3	-0.47	+0.12
4	-0.61	+0.11
5	-0.50	+0.12
6	-0.70	+0.10
7	-0.84	+0.08
FcC≡CPh		+0.13
Cp(dppe)FeC≡CPh	-0.36	

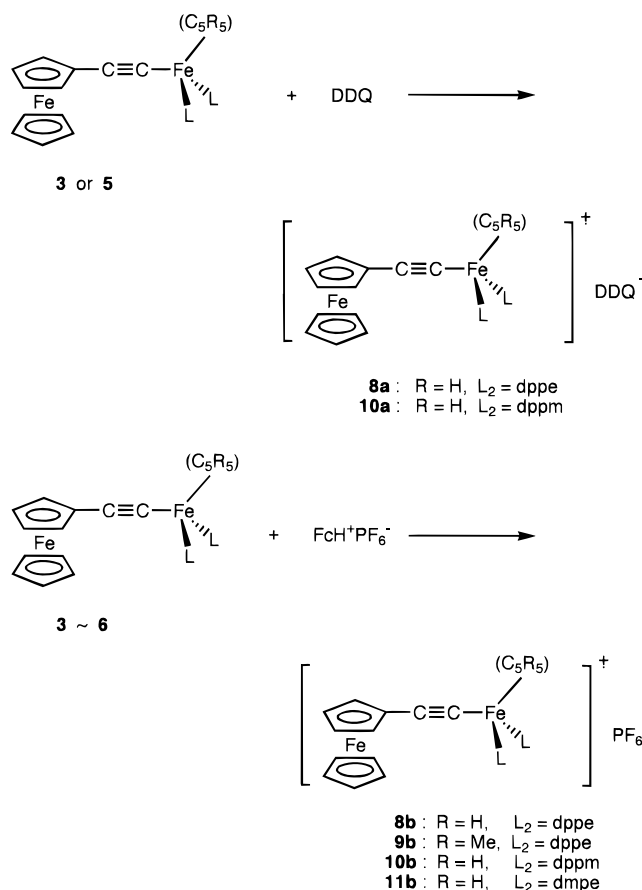
^a FcH/FcH⁺ couple: +0.18 V vs Ag/Ag⁺.

that in Cp(dppe)FeC≡CPh (74.8(2)°),¹² reflecting that the former contains a five-membered chelate ring but the latter a four-membered chelate ring. The Fe(1)–Fe(2) distance is 6.065 Å, which is similar to that in the Ru analog [Cp(Ph₃P)₂RuC≡CFc]PF₆.^{8a}

Redox Behavior. The redox behavior of **3**–**7** and the reference compounds was examined using cyclic voltammetry. All measurements were carried out at a scan rate of 100 mV s⁻¹ in a solution of 0.1 M (*n*-Bu)₄NClO₄ in acetonitrile, and the results are summarized in Table 2. For example, the cyclic voltammogram of **3** showed two quasi-reversible waves at *E*_{1/2} = -0.47 and +0.12 V (vs FcH/FcH⁺). The lower potential wave is assigned to the redox wave of the Cp(dppe)Fe– moiety and the other to the ferrocenyl moiety. These assignments are based on the reference compounds Cp(dppe)FeC≡CPh and ferrocenylphenylacetylene which gave reversible waves at *E*_{1/2} = -0.36 and +0.13 V, respectively. Complexes **4**–**7** also showed behavior similar to that of **3**. The redox potentials in these complexes are strongly influenced by the type of ligands around the Fe(II) atom. In a comparison of complexes **4** and **7** with **3** and **6**, respectively, the replacement of the Cp ligand by the Cp* ligand results in the shift of the first redox potential to lower potential by 0.14 V. Furthermore, the first redox potential of the dmpe series (**6** and **7**) is lower by 0.23 V compared with that of the dppe series (**3** and **4**). This is probably due to the greater electron-donating capability of Cp* and dmpe ligands, compared with that of Cp and dppe ligands, respectively. In these complexes, a large difference was observed between the first and second redox potentials. Usually, Δ*E* can be used to calculate the comproportionation constant (*K*_c) according to eq 1, where Δ*E* = *E*_{1/2}(2) – *E*_{1/2}(1) (mV).¹⁵

$$K_c = \exp((\Delta E)F/RT) = \exp(\Delta E/25.69) \quad (1)$$

*K*_c calculated for complexes **3**–**7** is typically ≥10¹⁰, this result being mainly due to substantial redox dissymmetry rather than to delocalization. If the difference between the half-wave potentials of the reference compounds (e.g., Cp(CO)₂FeC≡CPh and FcC≡CPh) is subtracted from Δ*E* of complex **3** in order to compensate for the dissymmetry, the ΔΔ*E* value obtained may be used to calculate the constant *K*_c. The application of such a treatment to complex **2** afforded a *K*_c value of 3.9 × 10⁶ for **2**. This *K*_c value is near that calculated using the Δ*E* value reported for biferrocene (Fc–Fc), 9.3 × 10⁵, and is much larger than that for diferrocenylacetylene (FcC≡CFc), 1.6 × 10², whose one-electron-oxidized species is classified as a class II type of mixed-valence complex.¹⁶ This fact suggests the validity of

Scheme 2

such a treatment. However, the *K*_c value calculated for **3** by the above treatment is only 49, much smaller than that expected from other data (*vide infra*), indicating that the treatment described above is not appropriate for such a dissymmetric system or that an unknown factor lowers the *E*_{1/2}(2) value for **3**, resulting in the small *K*_c value.

Oxidative Behavior. The complexes **3** and **5** were oxidized with 1 equiv of DDQ (2,3-dichloro-5,6-dicyanobenzoquinone) (*E*_{1/2} = +0.14 V) in CH₂Cl₂/benzene to respectively give the one-electron-oxidized species **8a** and **10a** as stable compounds, at least in the solid state, in good yield. Similarly, oxidation of **3**–**6** with FcH⁺PF₆⁻ (*E*_{1/2} = 0.0 V) in CH₂Cl₂ gave the corresponding one-electron-oxidized products **8b**–**11b** in good yield, which were characterized by IR spectroscopy and elemental analysis. For example, the IR spectrum of **8a** showed the C≡N, C≡C, and C=O stretching frequencies at 2204, 1956, and 1580 cm⁻¹, respectively.

Near-Infrared Spectra. All oxidized complexes described above showed a broad absorption in the near-IR region. The near-IR spectra of **8a** and **10a**, along with those of **1a** and **2a**, are shown in Figure 2, and the near-IR spectral data are summarized in Table 3. Meyer et al.¹⁷ reported that in the case of the near-IR bands observed for the mixed-valence complexes [Fc–Fc]⁺ and [FcC≡CFc]⁺ their transition energy (*ν*_{max}) was proportional to the solvent dielectric function, 1/*D*_{op}² – 1/*D*_s, where *D*_{op} and *D*_s are optical and statistical dielectric constants of the solvent involved, respectively.

(16) Le Vanda, C.; Bechgaard, K.; Cowan, D. C. *J. Organomet. Chem.* **1976**, *41*, 2700.

(17) Powers, M. J.; Meyer, T. J. *J. Am. Chem. Soc.* **1978**, *100*, 4393.

(15) Richardson, D. E.; Taube, H. *Inorg. Chem.* **1981**, *20*, 1278.

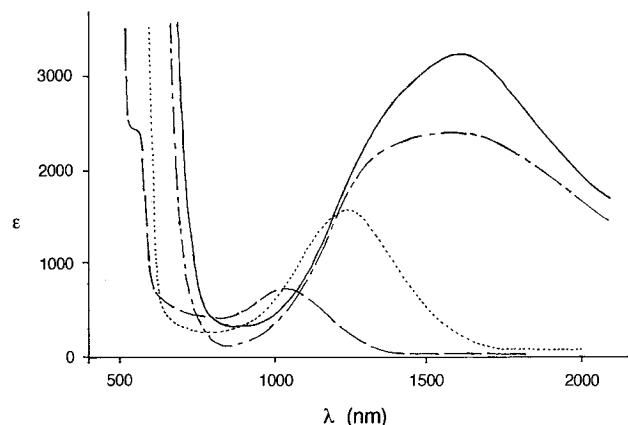


Figure 2. Near-IR spectra of **1a** (---), **2a** (···), **8a** (—), and **10a** (- - -) in CH_2Cl_2 .

Table 3. Near-IR Spectral Data for Complexes **8–11**

compd	solvent	$1/D_{\text{op}}^2 - 1/D_s^a$	λ_{max} (nm)	ν_{max} (10^3 cm^{-1})	ϵ_{max}	α^2 ($\times 10^{-2}$)
8a	CH_2Cl_2	0.380	1590	6.29	3060	2.31
	CD_2Cl_2	0.382	1590	6.29	2240	1.96
	CH_3NO_2	0.489	1510	6.62	2690	2.25
	CH_3COCH_3	0.496	1470	6.80	2370	1.85
	CH_3CN	0.526	1470	6.80	2150	1.80
8b	CH_2Cl_2		1590	6.29	3400	2.44
10a	CH_2Cl_2		1595	6.27	2260	1.98
10b	CH_2Cl_2		1595	6.27	2700	2.26
11b	CH_2Cl_2		1295	7.72	1630	0.98

^a Reference 14.

According to the Hush theory, the mixed-valence complexes display low-energy (near-IR) absorption bands which are assigned to intervalence transfer (IT) transition and exhibit the solvent effect described above. As shown in Table 3 and Figure 3, a linear correlation is observed between ν_{max} of complex **8a** and $1/D_{\text{op}}^2 - 1/D_s$ of the solvent used, reasonably meaning that the near-IR bands of the one-electron-oxidized complexes **8–11** can be assigned as the IT band of mixed-valence complexes. The linear slope ($3.7 \times 10^3 \text{ cm}^{-1}$) for **8a** in Figure 3 is smaller than that ($4.4 \times 10^3 \text{ cm}^{-1}$) found for the one-electron-oxidized species (**1a**) of **1**.⁷ It has been reported that the stabilization of a mixed-valence complex by solvation is strongly dependent on the extent of electron delocalization in the system. The larger the interaction between the metals in the mixed-valence complex was, the smaller the influence of solvent on the IT band became.^{3d,17} Thus, complexes **8–11**, with a phosphine ligand, seem to have a greater interaction between the two iron atoms than the carbonyl analog **1a**. Then, the interaction parameter α^2 , which gives an approximate measure for the degree of ground-state delocalization in a mixed-valence complex, was calculated for complexes **8–11** using eq 2, where $\Delta\nu_{1/2}$ is the

$$\alpha^2 = [(4.2 \times 10^{-4})\epsilon_{\text{max}}\Delta\nu_{1/2}]/\nu_{\text{max}}d^2 \quad (2)$$

half-width of the IT absorption band and d is the intermetallic distance.¹⁸ In this case, the internuclear distance (6.065(3) Å) observed for complex **3** was used as the value of d . The results are summarized in Table 3, along with the values of λ_{max} , ν_{max} , and ϵ_{max} . The values of α^2 for **8–11** are much larger than those of the

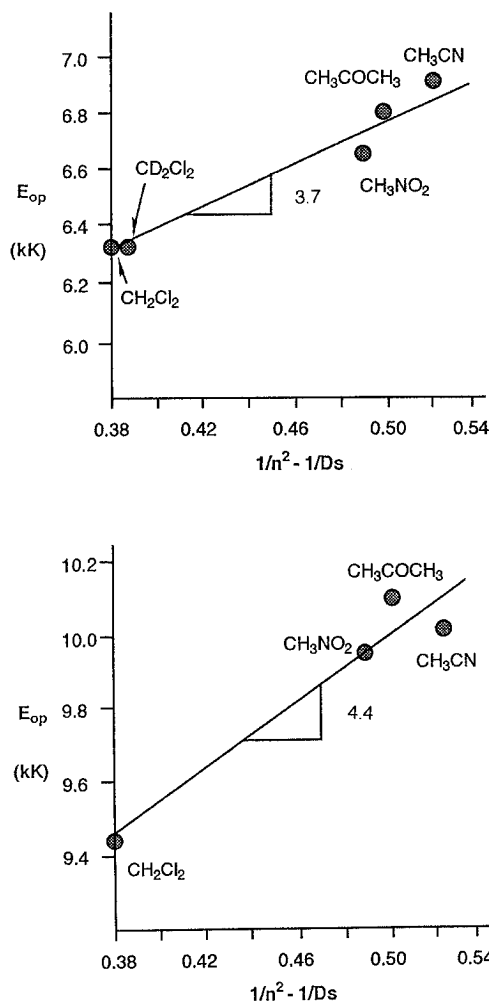


Figure 3. Plots of ν_{max} for **8a** (upper) and **1a** (bottom) vs $1/D_{\text{op}}^2 - 1/D_s$ for the solvent used.

analogous carbonyl complexes (e.g. $\alpha^2 < 6.4 \times 10^{-3}$).⁷ This suggests that there is greater electron delocalization between two Fe centers in the phosphine complexes **8–11** than in the carbonyl complexes, which is consistent with the consideration from the solvent effect described above. The large electron delocalization in the oxidized species (**8–11**) of the phosphine complexes **3–6** compared with that of the carbonyl complex **1** may be explained as follows. The MO calculation¹⁹ and the PE spectrum of $\text{Cp}(\text{CO})_2\text{FeC}\equiv\text{CR}$ ²⁰ indicate that the HOMO is an essentially metal-based orbital mixed with the acetylenic π bond. In other words, the d orbital on the Fe atom in the $\text{Cp}(\text{CO})_2\text{Fe}$ part can easily interact with the acetylenic π orbital. This seems to be the case in the complex $\text{Cp}(\text{Ph}_3\text{P})_2\text{FeC}\equiv\text{CR}$. In ferrocene, the e_{1g} (or e_{1u}) orbital of the Cp ligand which can interact with the acetylenic π orbital forms the molecular orbital by coupling with the d_{xz} or d_{yz} orbital of the iron atom, but this orbital is not the HOMO.²¹ As shown by the CV measurement, the first oxidized site of **3** is the $\text{Cp}(\text{dppe})_2\text{Fe}$ part (*vide supra*). Therefore, it is suggested that in the oxidized species of **3** the unpaired electron is easily delocalized into the acetylenic π bond, because

(19) Kostic, N. M.; Fenske, R. F. *Organometallics* **1982**, *1*, 974.

(20) Lichtenberger, D. L.; Renshaw, S. K.; Bullock, R. M. *J. Am. Chem. Soc.* **1993**, *115*, 3276.

(21) (a) Lauher, J. W.; Hoffmann, R. *J. Am. Chem. Soc.* **1976**, *98*, 1729. (b) Evans, E.; Green, M. L. H.; Jewitt, B.; Orchard, A. F.; Pygall, C. F. *J. Chem. Soc., Faraday Trans. 2* **1972**, *68*, 1847.

(18) (a) Hush, N. S. *Prog. Inorg. Chem.* **1967**, *8*, 391. (b) Creutz, C. *Prog. Inorg. Chem.* **1983**, *28*, 1.

the HOMO is the mixed orbital between the metal d orbital and the acetylenic π orbital, and then into the Fe atom of the ferrocene moiety through the e_{1g} (or e_{1u}) MO. In agreement with this idea, the STO-3G calculation using the Gaussian software package²² for $\text{Cp}(\text{PH}_3)_2\text{FeC}\equiv\text{CFc}$ (**3'**) in which the atomic coordinates in the molecule are based on those of the X-ray analysis of the complex **3** showed a remarkable contribution of the metal d orbital of the $\text{Cp}(\text{PH}_3)_2\text{Fe}-$ part to the HOMO in molecule **3'**. The NBO charges²³ of +1.53 and +1.39 on the Fe atoms in the Fc and $\text{Cp}(\text{PH}_3)_2\text{Fe}$ parts in the molecule **3'**, respectively, suggest that the electron is removed from the $\text{Cp}(\text{PH}_3)_2\text{Fe}-$ site and can be delocalized to the Fc part. On the other hand, according to the CV measurement, the first oxidized site of carbonyl complex **1** is the Fc part. That is, the electron is removed from the HOMO of ferrocene (a $d_{x^2-y^2}$ orbital of e_{2g} symmetry).²⁴ In the oxidized species of **1** the unpaired electron generated in the ferrocene moiety is considered to be difficult to delocalize to the acetylenic π bond because the HOMO is a $d_{x^2-y^2}$ orbital which interacts very little with a d_{xz} or d_{yz} orbital of e_{1g} symmetry. Therefore, the unpaired electron on the Fe atom in the Fc part can scarcely be delocalized to the Fe atom in the $\text{Cp}(\text{CO})_2\text{Fe}$ part in **1**. Thus, the electron delocalization in the oxidized species of **3** seems to be due to electron removal from the metal d orbital in the $\text{Cp}(\text{Ph}_3)_2\text{Fe}$ part coupled with the acetylenic π orbital and effective conjugation with the e_{1g} orbital of the Cp ligand coupled with the d_{xy} or d_{xz} orbital of the Fe atom in the ferrocene moiety. A comparable electron delocalization observed in $\text{Cp}(\text{Ph}_3\text{P})_2\text{RuC}\equiv\text{CFc}$ seems to be explicable similarly.^{8a} Also, an increase of the electron density in the whole system through the displacement of CO by the phosphine ligand may contribute to the electron delocalization by the stabilization of the radical cation formed. As a supporting fact, the electron delocalization increased linearly with the electron donating ability of the substituents in the Pt(II) analogs $\text{FcC}\equiv\text{CPt}(\text{PPh}_3)_2(\text{C}_6\text{H}_4\text{-X-p})$.^{8c} Complex **11** with the dmpe ligand, which has the strongest s-donating ability of the diphosphine ligands used, shows a value of α^2 rather smaller than the others. This phenomenon cannot be elucidated clearly at present but seems to suggest the importance of factors other than the electronic effect (e.g., the remarkable dissymmetry in the electronic structure ($\Delta E = 0.8$ V) may be concerned with the IT transition between the metals in this kind of oxidized complex). The α^2 values observed in **8–11** are also considerably larger than those for the oxidized species of other binuclear complexes which have a similar internuclear distance and are classified as class II mixed-valence complexes: 2.4×10^{-3} in $[\text{FcC}\equiv\text{CFc}]\text{-PF}_6$,¹⁷ 2.3×10^{-3} in $[\text{FcC}\equiv\text{NRu}(\text{NH}_3)_5](\text{PF}_6)_3$,²⁵ and 2.7×10^{-3} in $[\text{FcC}\equiv\text{CCC}_6\text{O}_3(\text{CO})_6\text{L}_3]\text{BF}_4$.²⁶ This suggests

Table 4. IR Spectral Data for Complexes 8–11

compd	ν_{CC} (cm^{-1})	$\Delta\nu^a$	compd	ν_{CC} (cm^{-1})	$\Delta\nu^a$
8a	1956	116	10a	1966	98
8b	1960	112	10b	1970	94
9b	1964	96	11b	1976	76

^a The difference between the neutral and the oxidized species.

that a facile electron transfer takes place between the two metal sites in complexes **8–11**, as well as in the analogous complex $[\text{FcC}\equiv\text{CRu}(\text{PPh}_3)_2(\eta\text{-C}_5\text{H}_5)]\text{BF}_4$ ($\alpha^2 = 1.3 \times 10^{-2}$).^{8a}

Hush has shown that the half-width ($\Delta\nu_{1/2}$) and the peak position (ν_{max}) of the IT absorption can be used to evaluate the zero-point energy difference (ν_0) and the thermal energy barrier (E_{th}) between metal sites in a mixed-valence complex (ν in 10^3 cm^{-1} and $T = 300 \text{ K}$):

$$\begin{aligned}\nu_0 &= \nu_{\text{max}} - [(\Delta\nu_{1/2})^2/16kT\ln 2] \\ &= \nu_{\text{max}} - [(\Delta\nu_{1/2})^2/2.13]\end{aligned}\quad (3)$$

$$E_{\text{th}} = [(\nu_{\text{max}})^2/4(\nu_{\text{max}} - \nu_0)] \quad (4)$$

Furthermore, according to Brown's proposal,²⁷ the thermal rate constant (k_{th}) for thermal electron transfer between the metal sites separated by a thermal energy barrier (E_{th}) is approximated as follows:

$$k_{\text{th}} = (kT/h) \exp(-E_{\text{th}}/RT) \quad (5)$$

The values of k_{th} for the electron transfer in the oxidized complexes **8–11** were calculated using the eqs 3–5 in turn. These values in CH_2Cl_2 were given as follows: **8a**, $9.1 \times 10^9 \text{ s}^{-1}$; **8b**, $4.4 \times 10^9 \text{ s}^{-1}$; **10a**, $5.0 \times 10^{10} \text{ s}^{-1}$; **10b**, $3.1 \times 10^{10} \text{ s}^{-1}$; **11b**, $4.2 \times 10^8 \text{ s}^{-1}$. However, the value of E_{th} obtained by eq 3 actually can become smaller because the coupling energy H_{ab} is neglected in Hush's model and, therefore, electron-transfer of **8–11** in CH_2Cl_2 probably occurs at a faster rate than the k_{th} stated above (e.g. **8** and **10**, $\geq 10^{11} \text{ s}^{-1}$; **11**, $\geq 10^9 \text{ s}^{-1}$). In any case, this suggests that the electron is transferred at a very fast rate between the metal nuclei in these complexes, although the rate for thermal electron transfer is somewhat smaller than that for nuclear frequency (10^{12} s^{-1}). That is, the electron is delocalized, in an unequal but certain ratio, between two iron atoms. Thus, complexes **8–11** can be considered to be mixed-valence complexes close to a type of class III.

Infrared Spectra. The IR spectral data are summarized in Table 4. The absorptions assigned to the $\text{C}\equiv\text{C}$ stretching vibration in the one-electron-oxidized complexes **8–11** were observed near 1960 cm^{-1} as a strong and broad band. This is in striking contrast to the weak and sharp absorption observed at $2050\text{--}2070 \text{ cm}^{-1}$ for the neutral complexes **3–7**, and the position is about intermediate between that of the neutral species and the allenylidene complex, $[\text{Ru}(\text{C}\equiv\text{C}-\text{Ph})_2(\text{PMe}_3)_2\text{Cp}]\text{PF}_6$ (**12**; 1926 cm^{-1}).²⁸ If electron transfer between two metal sites takes place faster than on the IR time scale (10^{12} s^{-1}), only one absorption band averaged between the two limiting species **A** and **B** should be observed for the $\text{C}\equiv\text{C}$ stretching vibration.

(22) Frish, M. J.; Trucks, G. M.; Head-Gordon, M.; Gill, P. M.; Gill, P. M. W.; Wong, M. W.; Foresman, J. B.; Johnson, B. G.; Schlegel, H. B.; Robb, M. A.; Replogle, E. S.; Gompert, R.; Andres, J. L.; Raghavachari, K.; Binkley, J. S.; Gonzalez, C.; Martin, R. L.; Fox, D. J.; Defrees, D. J.; Baker, J.; Stewart, J. J. P.; Pople, J. A. Gaussian 92, Revision D.3; Gaussian Inc.: Pittsburgh, PA, 1992.

(23) Read, A. E.; Weinstock, R. B.; Weinhold, F. *J. Chem. Phys.* **1985**, *83*, 735.

(24) Prins, R. *Mol. Phys.* **1970**, *19*, 603.

(25) Dowling, N.; Henry, P. M.; Lewis, N. A.; Taube, H. *Inorg. Chem.* **1981**, *20*, 2345.

(26) Kotz, J.; Neyhart, G.; Vining, W. J.; Rausch, M. D. *Organometallics* **1983**, *2*, 79.

(27) Brown, G. M.; Sutin, N. *J. Am. Chem. Soc.* **1979**, *101*, 883.

(28) Selegue, J. P. *Organometallics* **1982**, *1*, 217.

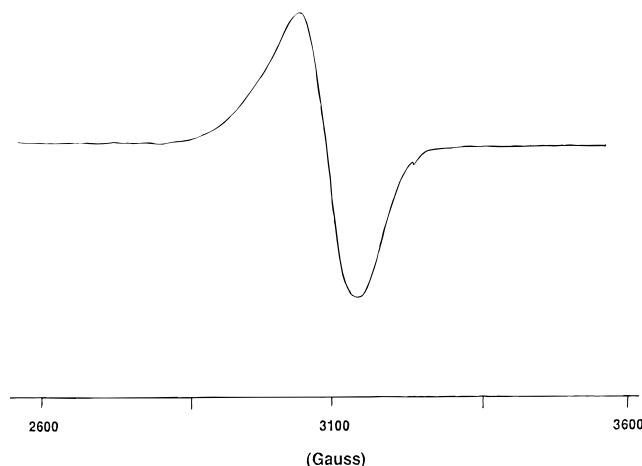
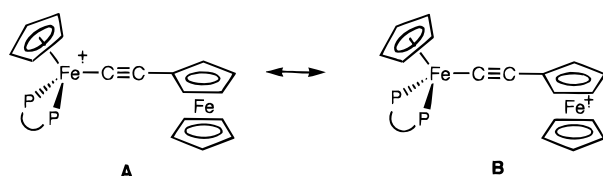


Figure 4. ESR spectrum of **8a** in CH_2Cl_2 at 5.5 K.

Scheme 3



Recently, it was reported that the value of ν_{CC} , accompanying the conversion of the $\text{MC}\equiv\text{CC}\equiv\text{CM}$ complex to its one-electron-oxidized species, was shifted to an averaged frequency between the neutral and the dioxidized species because of the rapid electron transfer ($>10^{12} \text{ s}^{-1}$) in the system.^{4c,29} Complexes **8–11** exhibited a similar shift of ν_{CC} to lower wavenumber by ca. 100 cm^{-1} . This may suggest that the electron transfer between the two Fe atoms is very rapid, on the IR time scale. However, we could not confirm this possibility, since the dioxidized species of complexes **3–7** were not available because of their instability. The shift to lower wavenumber from the corresponding neutral complex decreased in the following order: **8** > **9** > **10** > **11**. This order is parallel to that of the rate of thermal electron transfer calculated from the near-IR spectral data. Therefore, the IR spectral data also seem to support the suggestion from the near-IR spectra that complexes **8–11** may be classified as the mixed-valence type close to a type of class III.

ESR Spectra. The ESR spectra of **8a** were measured in both the solid state and CH_2Cl_2 solution at 5.5 K and room temperature. However, in either case only one signal with a width of ca. 1000 G was observed, as shown in Figure 4. This is in great contrast to the case of the carbonyl complex **1a**, which showed two signals at $g_{\parallel} = 3.81$ and $g_{\perp} = 1.68$, suggesting localization of the radical cation on its ferrocenyl part.⁷ According to the result obtained in cyclic voltammetry, the first oxidation site in complex **3** is the CpFeP_2 part. If the radical cation is localized there on the ESR time scale (10^{-9} s), anisotropy of the g value (two g values, as for $\text{FeCp}^*(\text{dppe})\text{Me}^+$) ought to be observed in complex **8**, because an Fe(III) half-sandwich complex has axis symmetry.³⁰ As seen clearly in Figure 4, only one signal with $g = 2.09$ appeared in the ESR spectrum of complex

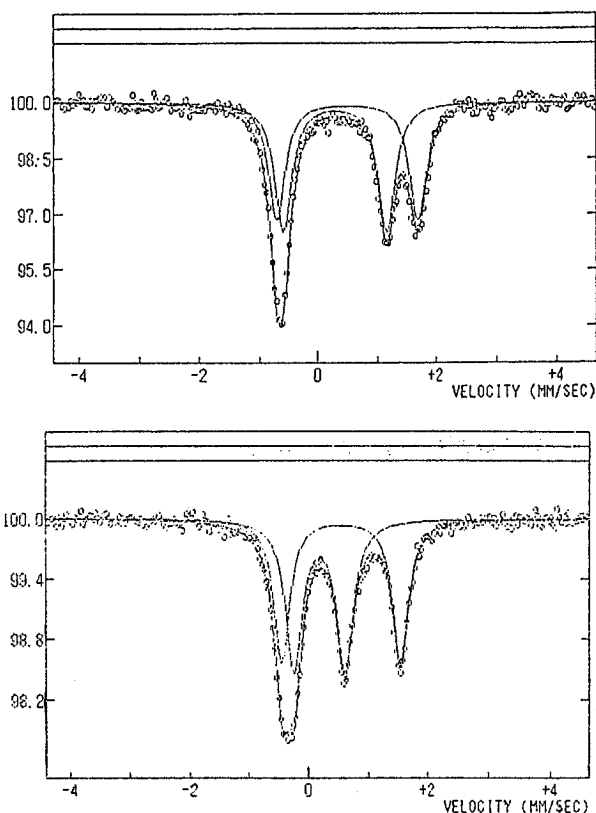


Figure 5. Mössbauer spectra of **3** (upper) and **8b** (bottom).

Table 5. Mössbauer Parameters for Complexes **3**, **6**, and **8–11**

compd	IS (mm s^{-1})	QS (mm s^{-1})	compd	IS (mm s^{-1})	QS (mm s^{-1})
3	0.28	1.77	9b	0.25	0.96
	0.49	2.41		0.53	2.19
6	0.23	1.77	10b	0.15	0.91
	0.54	2.40		0.53	2.22
8b	0.19	0.86	11b	0.15	1.00
	0.55	2.00		0.53	2.26

8. We also observed no temperature dependence in the ESR spectra of **8**. Therefore, it is considered that the rate of the electron transfer in **8** is faster than 10^{-9} s even at 5.5 K. This result seems to be consistent with the IR and near-IR spectral data. The small signal near 3250 G is probably due to the DDQ radical anion.

Mössbauer Spectra. The Mössbauer spectra of **3**, **6**, and **8–11** were measured at 77 K, and the results are summarized in Table 5. The spectra of the neutral complex **3** and the oxidized complex **8b** are shown in Figure 5. In the spectra of **3** and **6** two doublets were observed, whose QS values are consistent with those of ferrocene derivatives (ca. 2.42 mm s^{-1}) and a half-sandwich complex, $\text{Cp}^*(\text{dppe})\text{FeMe}$ (1.82 mm s^{-1}).³⁰ These indicate that two Fe(II) atoms exist in complexes **3** and **6**. On the other hand, in the one-electron-oxidized complex **8b**, two doublets with QS = 0.86 and 2.00 mm s^{-1} were observed, as seen in Figure 5. In comparison with the reference complex, $[\text{Cp}^*(\text{dppe})\text{FeMe}]\text{PF}_6$ (0.76 mm s^{-1}),³⁰ the doublet of QS = 0.86 mm s^{-1} is assigned to the half-sandwich unit in **8b**. This confirms that the oxidized site in **8** is the iron atom in the half-sandwich unit, not the one in the ferrocenyl part, as well as the above-mentioned discussions. The QS value (2.00 mm s^{-1}) of the doublet due to the ferrocenyl moiety is smaller than that (2.41 mm s^{-1}) of the neutral complex **3**. Such

(29) Seyler, J. W.; Weng, W.; Zhou, Y.; Gladysz, J. A. *Organometallics* **1993**, *12*, 3802.

(30) Roger, C.; Hamon, P.; Toupet, L.; Rabaa, H.; Saillard, J.-Y.; Hamon, J.-R.; Lapinte, C. *Organometallics* **1991**, *10*, 1045.

a low value for a neutral ferrocene derivative is unprecedented. This may be explained as follows: the fast electron transfer between two iron atoms occurs over the time scale of the Mössbauer measurement (10^{-7} s) in complex **8b**, so that the QS value of the iron atom in both sites approaches the averaged value. That is, the QS value of the neutral site decreases and that of the radical cation site increases. In fact, such a tendency was observed in the monocations of [0.0]ferrocenophane (QS = 1.78 mm s^{-1}),³¹ [2.2]ferrocenophane-1,13-diyne (QS = 1.61 mm s^{-1}),³¹ and $[\text{Cp}^*(\text{dppe})\text{Fe}]_2\text{C}_4$ (QS = 1.32 mm s^{-1}),^{4c} which were classified as class III mixed-valence complexes. However, this explanation is somewhat uncertain, because the QS value (0.86 mm s^{-1}) of the $\text{Cp}(\text{dppe})\text{Fe}$ site in complex **3** is rather close to that (0.76 mm s^{-1}) of the reference complex $[\text{Cp}^*(\text{dppe})\text{FeMe}]\text{PF}_6$.³⁰ Complete averaging of the QS values of two iron sites may not appear in a dissymmetric molecule even if a fast electron transfer exists between the metal sites. While the near-IR data of complex **10** are indicative of the existence of fast electron transfer as in complex **8**, the QS value (2.22) of **10b** is relatively larger than that of **8b**. For the present, we suppose that it is due to the structural strain at the methylene moiety of dpmm in the solid state.

Summary. Some Fe(II) ferrocenylacetylide complexes with a diphosphine ligand were prepared by photolysis of the corresponding carbonyl complexes in the presence of the diphosphines in excellent yield. Their one-electron oxidation provided a new type of mixed-valence complex. The one-electron-oxidized complexes **8–11** showed behavior close to class III of mixed-valence compounds in all measurements (IR, near-IR, ESR, and Mössbauer spectra). In dissymmetric complexes, to the best of our knowledge, there are few instances that have as large an electron delocalization as in complexes **8–11**.

Experimental Section

Visible and near-infrared spectra were recorded on a Shimadzu 365 spectrometer and IR spectra on a Hitachi 270-50 spectrometer. ^1H and ^{13}C NMR spectra were measured on a Bruker AM400 spectrometer. Electrochemical measurements were made by cyclic voltammetry in a solution of 0.1 M (*n*-Bu)₄NClO₄ in CH_2Cl_2 or acetonitrile under nitrogen at 25 °C, using a standard three-electrode cell on a BAS CV-27 analyzer. All potentials were measured vs a Ag/AgNO_3 (0.05 M) electrode, and the scan rate was 100 mV/s. ESR spectra were measured on a JEOL JES-PE-3X spectrometer. Mössbauer spectra were measured with a constant-acceleration type spectrometer, and the velocity scale was calibrated on the spectrum of metallic iron at room temperature. Spectra were fitted with Lorentzian line shapes by least squares. The isomer shifts were reported with respect to α -Fe foil at room temperature. The error of the values of isomer shift and quadrupole splitting was estimated as within $\pm 0.02 \text{ mm s}^{-1}$.

Ferrocenylacetylene,³² $(\eta\text{-C}_5\text{H}_5)(\text{CO})_2\text{FeI}$,³³ $(\eta\text{-C}_5\text{Me}_5)(\text{CO})_2\text{FeI}$,³⁴ $(\eta\text{-C}_5\text{H}_5)(\text{CO})_2\text{FeC}\equiv\text{Cfc}$ (**1**), and $(\eta\text{-C}_5\text{Me}_5)(\text{CO})_2\text{FeC}\equiv\text{Cfc}$

(**2**)⁷ were prepared according to the methods described in the literature. All experiments were performed in a nitrogen-saturated solvent under nitrogen.

($\eta\text{-C}_5\text{H}_5$)(dppe)FeC≡Cfc (3). (a) A solution of complex **1** (50 mg, 0.13 mmol) and dppe (55 mg, 0.14 mmol) in acetonitrile (40 mL) was irradiated with a 100 W high-pressure Hg lamp for 30 min at 0 °C under bubbling of nitrogen. After the solution had been concentrated to a small volume, it was filtered. The filtrate was evaporated, and the residue was recrystallized from CH_2Cl_2 /hexane: red crystals (67 mg, 71%); mp 207 °C. Anal. Calcd for $\text{C}_{43}\text{H}_{38}\text{P}_2\text{Fe}_2$: C, 70.90; H, 5.25. Found: C, 70.67; H, 5.33. IR (KBr): 2072 cm^{-1} . ^1H NMR (CDCl_3): δ 2.31 (m, 2H, CH_2), 2.76 (m, 2H, CH_2), 3.76 (s, 2H, Fc), 3.67 (s, 5H, Fc unsub), 3.62 (s, 2H, Fc), 7.24–8.0 (m, 20H, Ph). ^{13}C NMR (CDCl_3): δ 28.57 (t, $J = 24.1 \text{ Hz}$, CH_2), 65.63 (Fc), 66.51 (Fc unsub), 69.24 (Fc), 70.02 (Fc ipso), 79.00 ($\eta\text{-C}_5\text{H}_5$), 127.48, 127.66 (Ph *p*), 128.62, 129.13 (Ph *m*), 131.70, 134.08 (Ph *o*), 138.02 (t, $J = 23 \text{ Hz}$, Ph ipso), 142.44 (m, Ph ipso).

(b) Ferrocenylacetylene (84 mg, 0.4 mmol) and $(\eta\text{-C}_5\text{H}_5)(\text{dppe})\text{FeI}$ (150 mg, 0.23 mmol) were dissolved in dry THF (3 mL) under nitrogen, and the solution was chilled in an ice-water bath. To the solution was slowly added methyllithium (0.8 mL of 1.4 M solution in diethyl ether, 1.12 mmol). After it was stirred for 15 min, the solution was evaporated. The residue was chromatographed on deactivated alumina to give the title complex (107 mg, 64%) as red crystals after recrystallization from CH_2Cl_2 /hexane: mp 207 °C.

($\eta\text{-C}_5\text{H}_5$)(dpmm)FeC≡Cfc (5). This complex was prepared in a method similar to that used for complex **3**: red crystals (64%); mp 170–180 °C dec. Anal. Calcd for $\text{C}_{42}\text{H}_{36}\text{P}_2\text{Fe}_2$: C, 70.61; H, 5.07. Found: C, 70.41; H, 5.09. IR (KBr): 2064 cm^{-1} ($\text{C}\equiv\text{C}$). ^1H NMR (CDCl_3): δ 3.92 (m, 2H, CH_2), 3.40 (bs, 2H, Fc), 3.58 (s, 5H, Fc unsub), 3.71 (bs, 2H, Fc), 4.39 (s, 5H, $\eta\text{-C}_5\text{H}_5$), 7.26–7.80 (m, 20H, Ph). ^{13}C NMR (CDCl_3): δ 44.26 (CH_2), 65.85 (Fc β), 68.50 (Fc unsub), 69.94 (Fc α), 76.47 ($\eta\text{-C}_5\text{H}_5$), 127.75–139.10 (Ph).

($\eta\text{-C}_5\text{H}_5$)(dmpe)FeC≡Cfc (6). This complex was prepared in a similar manner. Crystallization from ether/hexane provided complex **6** as an orange powder (80%); Mp 160–162 °C dec. Anal. Calcd for $\text{C}_{23}\text{H}_{30}\text{P}_2\text{Fe}_2$: C, 57.53; H, 6.29. Found: C, 57.07; H, 6.48. IR (KBr): 2052 cm^{-1} ($\text{C}\equiv\text{C}$). ^1H NMR (CDCl_3): δ 1.45, 1.75 (bs, 12H, CH_3), 1.62, 1.95 (m, 4H, CH_2), 3.91 (bs, 2H, Fc), 4.05 (bs, 2H, Fc), 4.07 (s, 5H, Fc unsub), and 4.16 (s, 5H, $\eta\text{-C}_5\text{H}_5$). ^{13}C NMR (CDCl_3): δ 19.09, 20.56 (CH_3), 29.42 (CH_2), 66.40 (Fc β), 69.42 (Fc unsub), 69.82 (Fc α), 77.05 ($\eta\text{-C}_5\text{H}_5$), 77.39, 110.42 ($\text{C}\equiv\text{C}$).

($\eta\text{-C}_5\text{Me}_5$)(dppe)FeC≡Cfc (4). A solution of complex **2** (50 mg, 0.11 mmol) and dppe (44 mg, 0.11 mmol) in diethyl ether (20 mL) and hexane (20 mL) was irradiated with the same lamp used in the Cp series for 15 min at 0 °C under bubbling of nitrogen. The solution was purified in a manner similar to that used for complex **3**: red-orange crystals (54 mg, 62%); mp 207 °C dec. Anal. Calcd for $\text{C}_{48}\text{H}_{48}\text{P}_2\text{Fe}_2$: C, 72.19; H, 6.05. Found: C, 71.95; H, 6.28. IR (KBr): 2060 cm^{-1} ($\text{C}\equiv\text{C}$). ^1H NMR (CDCl_3): δ 1.32 (s, 15H, $\eta\text{-C}_5\text{Me}_5$), 1.92, 2.73 (m, 4H, CH_2), 3.89 (bs, 2H, Fc), 3.91 (s, 5H, Fc unsub), 3.98 (bs, 2H, Fc), 7.24–7.96 (m, 20H, Ph). ^{13}C NMR (CDCl_3): δ 9.84 ($\eta\text{-C}_5\text{Me}_5$), 88.28 ($\eta\text{-C}_5\text{Me}_5$), 27.60 (CH_2), 66.98 (Fc β), 68.74 (Fc unsub), 72.00 (Fc α), 127.09–138.69 (Ph).

($\eta\text{-C}_5\text{Me}_5$)(dmpe)FeC≡Cfc (7). This complex was similarly prepared in acetonitrile and crystallized from diethyl ether/hexane at -78 °C: orange powder (67%); mp 146 °C. Anal. Calcd for $\text{C}_{28}\text{H}_{40}\text{P}_2\text{Fe}_2$: C, 61.11; H, 7.32. Found: C, 60.81; H, 7.34. IR (KBr): 2044 cm^{-1} ($\text{C}\equiv\text{C}$). ^1H NMR (C_6D_6): δ 0.95, 1.49 (bs, 12H, CH_3), 1.75 (s, 15H, $\eta\text{-C}_5\text{Me}_5$), 1.03, 1.90 (m, 4H, CH_2), 3.98 (bs, 2H, Fc), 4.26 (s, 5H, Fc unsub), 4.29 (bs, 2H, Fc). ^{13}C NMR (C_6D_6): δ 11.10 ($\eta\text{-C}_5\text{Me}_5$), 88.28 ($\eta\text{-C}_5\text{Me}_5$), 16.84, 18.42 (CH_3), 30.02 (CH_2), 66.33 (Fc β), 69.37 (Fc unsub), 69.91 (Fc α), 70.51 (Fc ipso), and 77.50, 108.10 ($\text{C}\equiv\text{C}$).

$[(\eta\text{-C}_5\text{H}_5)(\text{dppe})\text{FeCCFc}]^+[\text{C}_6\text{H}_4\text{Cl}_2(\text{CN})_2]^-$ (8a). To a solution of complex **3** (60 mg, 0.082 mmol) in CH_2Cl_2 (1.5 mL)

(31) (a) Motoyama, I.; Watanabe, M.; Sano, H. *Chem. Lett.* **1978**, 513. (b) Kramer, J. A.; Hendrickson, D. N. *Inorg. Chem.* **1980**, *19*, 3330.

(32) (a) Schlögl, K.; Steyrer, W. *Monatsh. Chem.* **1965**, *96*, 1521. (b) Rosenblum, M.; Brawn, N.; Papenmeier, J.; Applebaum, M. *J. Organomet. Chem.* **1966**, *6*, 173.

(33) King, R. B. *Organometallic Synthesis*; Academic Press: New York, 1965; Vol. 1, p 175.

(34) Akita, M.; Terada, M.; Oyama, S.; Moro-oka, Y. *Organometallics* **1990**, *9*, 816.

and benzene (20 mL) was added slowly a solution of dichlorodicyanobenzoquinone (DDQ; 20 mg, 0.088 mmol, freshly recrystallized from CH_2Cl_2) in benzene (13 mL) on an ice-water bath under nitrogen. After the mixture was stirred for 15 min, dry hexane (50 mL) was added slowly to the solution. The resulting deep blue crystals were filtered quickly: yield 46 mg (59%); mp $\sim 150^\circ\text{C}$ dec. Anal. Calcd for $\text{C}_{51}\text{H}_{38}\text{Cl}_2\text{N}_2\text{O}_2\text{P}_2\text{Fe}_2 \cdot \frac{1}{2}\text{CH}_2\text{Cl}_2$: C, 61.98; H, 3.93; N, 2.80. Found: C, 61.80; H, 4.04; N, 2.86. IR (KBr): 1956 cm^{-1} . Vis-near-IR (CH_2Cl_2): 465 (ϵ 6710), 600 (8170), 1590 nm (2240).

$[(\eta\text{-C}_5\text{H}_5)(\text{dppm})\text{FeC}\equiv\text{CFC}]^+\text{DDQ}^-$ (10a). This complex was prepared from complex **5** by a method similar to that used for complex **8a**: 85% yield; mp ca. 150°C dec. Anal. Calcd for $\text{C}_{50}\text{H}_{36}\text{N}_2\text{O}_2\text{Cl}_2\text{P}_2\text{Fe}_2$: C, 63.79; H, 3.85; N, 2.98. Found: C, 63.93; H, 4.13; N, 2.92. IR (KBr): $2208\text{ (C}\equiv\text{N)}$, $1966\text{ cm}^{-1}\text{ (C}\equiv\text{C)}$. Vis-near-IR (CH_2Cl_2): 460 (ϵ 5380), 593 (7200), 1595 nm (2260).

$[(\eta\text{-C}_5\text{Me}_5)(\text{dppe})\text{FeC}\equiv\text{CFC}]^+\text{PF}_6^-$ (9b). Complex **4** (50 mg, 0.063 mmol) was dissolved in CH_2Cl_2 (2 mL) and cooled to -78°C . To this solution was slowly added a solution of $\text{FcH}^+\text{PF}_6^-$ (21 mg, 0.063 mmol) in CH_2Cl_2 (6 mL) under nitrogen. The mixture was stirred for 15 min and then concentrated under reduced pressure. The concentrated solution was cooled to -78°C again. After addition of hexane to the solution, the resulting deep blue precipitate was filtered: yield 38 mg (64%); mp ca. 150°C dec. Anal. Calcd for $\text{C}_{48}\text{H}_{48}\text{F}_6\text{P}_3\text{Fe}_2 \cdot \frac{1}{2}\text{CH}_2\text{Cl}_2$: C, 59.08; H, 5.00. Found: C, 59.16; H, 5.37. IR (KBr): $1964\text{ cm}^{-1}\text{ (C}\equiv\text{C)}$. Vis-near-IR (CH_2Cl_2): 410 (ϵ 1380), 610 (2320), 1250 (1490), 1700 nm (828 sh).

Synthesis of $[(\eta\text{-C}_5\text{H}_5)(\text{PP})\text{FeC}\equiv\text{CFC}]^+\text{PF}_6^-$ (8b, 10b, and 11b). These oxidized complexes were similarly prepared from the respective neutral complexes **3**, **5**, and **6** according to the method described above. Complex **11b** is unstable in hexane, and so ether was used instead.

8b (PP = dppe): 71% yield; mp ca. 150°C dec. Anal. Calcd for $\text{C}_{43}\text{H}_{48}\text{F}_6\text{P}_3\text{Fe}_2 \cdot \frac{1}{2}\text{CH}_2\text{Cl}_2$: C, 57.04; H, 4.29. Found: C, 57.38; H, 4.40. IR (KBr): $1960\text{ cm}^{-1}\text{ (C}\equiv\text{C)}$. Vis-near-IR (CH_2Cl_2): 450 (ϵ 1790), 634 (6290), 1590 nm (3400).

10b (PP = dppm): 94% yield; mp ca. 150°C dec. Anal. Calcd for $\text{C}_{42}\text{H}_{36}\text{F}_6\text{P}_3\text{Fe}_2$: C, 58.70; H, 4.22. Found: C, 58.51; H, 4.40. IR (KBr): $1970\text{ cm}^{-1}\text{ (C}\equiv\text{C)}$. Vis-near-IR (CH_2Cl_2): 647 (ϵ 6220), 1595 nm (2700).

11b (PP = dmpe): 94% yield; mp ca. 150°C dec. Anal. Calcd for $\text{C}_{23}\text{H}_{30}\text{F}_6\text{P}_3\text{Fe}_2$: C, 44.19; H, 4.84. Found: C, 44.20; H, 4.97. IR (KBr): $1976\text{ cm}^{-1}\text{ (C}\equiv\text{C)}$. Vis-near-IR (CH_2Cl_2): 590 (ϵ 3870), 1295 nm (1630).

Structure Determination. Crystal data for **3**: $\text{C}_{43}\text{H}_{38}\text{P}_2\text{Fe}_2$, fw 728.40, monoclinic, $P2_1/c$ (No. 14); $a = 17.190(3)\text{ \AA}$, $b = 19.756(2)\text{ \AA}$, $c = 21.851(4)\text{ \AA}$; $\beta = 107.703(2)^\circ$; $V = 7069.3\text{ \AA}^3$; $Z = 8$; $D_{\text{calc}} = 1.37\text{ g/cm}^3$; $\mu(\text{Mo K}\alpha) = 9.444\text{ cm}^{-1}$; $T = 298\text{ K}$; crystal size $0.26 \times 0.20 \times 0.18\text{ mm}$.

Oscillation and nonscreen Weissenberg photographs were recorded on the imaging plates on a Mac Science DIP3000 diffractometer with graphite-monochromated Mo K α radiation and an 18-kW rotating anode generator. Data reduction and determination of cell parameters were made by the MAC DENZO program system. Of 16 860 reflections collected, 16 437 reflections were unique, 7207 reflections of which with $I > 3.00\sigma(I)$ were used for refinement. The structure was solved by direct methods using SIR92 in the CRYSTAN-GM program system (software package for structure determination) and refined by a full-matrix least-squares procedure. Hydrogen atoms were not located. Anisotropic refinement for non-hydrogen atoms was carried out. $R = 0.088$ and $R_w = 0.090$.

Supporting Information Available: Tables giving crystal data and data collection and refinement details, atomic coordinates, bond distances and angles, torsion angles, thermal parameters, and least-squares planes and deviations therefrom and figures giving additional views and atom numbering for **3** (61 pages). Ordering information is given on any current masthead page.

OM950525D